Applied Energy 183 (2016) 399–407

Contents lists available at ScienceDirect

Applied Energy

journal homepage: www.elsevier.com/locate/apenergy

Performance assessment and productivity of a simple-type solar still integrated with nanocomposite energy storage system

Ashraf Elfasakhany

Department of Mechanical Engineering, Faculty of Engineering, Taif University, Box 888, Taif, Saudi Arabia

HIGHLIGHTS

- Performance and productivity of solar still at different configurations are studied.
- Using nanocomposite (NCPW) can enhance the storage capacity of paraffin wax (PW).
- The NCPW increased the productivity by 6%, compared to PW.
- The total melting time of NCPW was decreases by 7%, compared to PW.
- The peak temperature of NCPW exceeds that of PW.

ARTICLE INFO

Article history:
Received 31 August 2016
Accepted 1 September 2016

Keywords:
Paraffin wax
Copper nanocomposite
Experiments
Desalination
Productivity

ABSTRACT

Paraffin wax (PW) is one of promising solar energy storage materials in solar distillers because of its relatively large latent heat with a stable phase change process. However, paraffin's low thermal conductivity is a negative aspect for its efficient practice. In this study, adding nanomaterial to enhance paraffin's low thermal conductivity and its performance parameters is examined. Three cases have been investigated and compared to each others, case 1 without PW, case 2 with PW, and case 3 with copper-PW nanocomposite (NCPW). The results showed apparent advantage of nanocomposite on thermal conductivity of PW and that enhanced the heat energy storage and water productivity. The productivity increased by about 125% and 119% for cases 3 and 2, respectively, compared to case 1. The system working time extended during night by 5 h and 6 h at applying PW and NCPW, respectively. It was also shown that adding nanomaterials to PW can not only increase its thermal conductivity but also the system efficiency and thermal storage capacity.

1. Introduction

Fresh water is one of the necessities not only for drinking but also in all aspects of the life. Most of our available water sources, e.g., 97%, are saline and the existing fresh water is minor [1]. In order to cover the shortage of fresh water availability, desalination of saline water is carried out. The desalination process is applied using different energy sources, e.g., fossil fuels [2–4] or renewable energies [5,6]. In recent years, fossil fuels have been limited because of their environmental problems and depletion nature [7–14]. Renewable energy is increasable applied in the desalination applications instead. One of the common renewable energies for the desalination is solar energy. Many researchers agreed that solar desalination is currently one of the most widely accepted distillation plants [15]. Solar distillation offers the simplest and most attracted method, compared with other distillation methods [16]. However, one of the major problems of the solar desalination is the noncontinuous operation due to a lack of solar radiation during the nighttime and, in turn, shortage of fresh water supply [17–22]. Accordingly, the productivity of solar stills is much lower than other thermal desalination plants. Extensive researches have been examined different aspects to overcome such problem in solar stills [23–25]. One of the proposed solutions is to use a system for energy storage in solar distillation during sunset and then takes advantage of it during the night. Based on early research in this issue, there are two different thermal energy storage systems are currently in use: either sensible or latent heat system. The latent heat thermal energy storage system showed advantages over sensible storage one because of its large energy storage capacity per unit volume and almost constant temperature for charging and discharging processes [26]. The idea of the latent heat storage system (or phase change materials, PCMs) is that it has a high heat of

E-mail address: ashr12000@yahoo.com

http://dx.doi.org/10.1016/j.apenergy.2016.09.002
0306-2619/

fusion for which melting (solid to liquid) and freezing (liquid to solid), at a certain temperature range, is just equivalent to absorbing and releasing large amounts of energy for the desalination process at night [27–30].

When making a literature review on the outcome of the use of PCMs in solar distillation, considerable papers were found. In brief, Abdallah et al. [31] examined different heat energy storage materials on still's productivity, such as metallic coated sponge, uncoated sponge and black igneous rocks. The study concluded that the best storage material was uncoated sponge, followed by the black rocks and then coated sponges. Dashtban and Tabrizi [1] carried out a thermal analysis of PCM storage in a weir-type cascade solar still to enhance the water productivity. The study applied a heat storage system in a plate form and the results showed that the daily productivity of the still with and without PCM, respectively, was about 6.7 and 5.1 kg/m^2 day. Radhawan [32] studied performance of different solar stills with PCM and study concluded that the basin still with PCM is more efficient for water productivity. El-Sebaii et al. [33] studied the performances of single basin solar still and stepped solar still integrated with PCM and came up with the conclusion of high productivity of PCM still. Kurklu et al. [34] studied experimentally using of PCM integrated into solar collector to investigate the system performance on a 24 h basis and results indicated better efficiency of such still. Khalifa et al. [35] studied experimentally the using of circular pipe absorber integrated into paraffin wax; results indicated that the collector efficiency increased by 45–54%. Al-Hinti et al. [36] studied paraffin wax stored in a water storage tank instead of solar collector and results indicated that 55 °C and 30 °C of hot water temperatures are produced in the daytime and next morning, respectively. Bouadila et al. [37] examined of a solar water heater integrated with PCM in a configuration of rectangular cavity; resulted showed that the PCM extended the operation of the system after sunset by approximately 5 h and the system efficiency is increased by about 25–35%. Wei et al. [38] studied the capability of PCM as heat storage/supply capacity in four different shapes (sphere, cylinder, plate and tube) and results showed that the sphere is the best storage/supply thermal energy among other shapes. Shukla et al. [39] examined thermal cycling load on different types of phase change materials (organic and inorganic types); they came up with that the organic PCMs were found workable up to 1000 thermal cycles, but inorganic PCMs were unable to properly work after little cycles. In a more recent study, Elfasakhany et al. [40] investigated experimentally the use of PCM in a simple type solar still and compared results without PCM condition. The results indicated that the case with PCM showed higher water productivity.

There are different materials could be used as PCMs, as shown from the above literatures. Paraffin wax (PW) is one the best promising PCM materials for the desalination process [41–44]. Paraffin wax (straight n-alkane or C_nH_{2n+2} chains) is superior because it has a high meting point with a fluent heat of fusion; its low vapor pressure, self-nucleating behavior, and commercial availability at low cost are extra advantages. However, one of major inhibition of the paraffin wax as storage material is its low thermal conductivity. The low thermal conductivity (about 0.17 W/m K [27]) limits its rate for the thermal storage and release of energy. To overcome this issue, different methods have been proposed; such methods can be classified into two main techniques: firstly, enlarging the heat transfer area by using heat exchanger with finned configuration; the results of this technique are encouraging, but limitations are noticed due to the increase in weight and volume of the storage system. The second technique is by enhancing the thermal conductivity of PW by using additives. The potential additives generally include dispersing metal particles [45,46], micro encapsulated materials [47,48], porous metallic matrix [49,50], porous graphite matrix [51,52], carbon nanotube [53,54], and carbon fibers [55,56]. The additive can enhance the thermal conductivity of PW and in the following a short summary from literature is presented. Ho and Gao [57] studied the effects of inserting alumina nanoparticles (5 wt.% and 10 wt.%) into a paraffin wax. The results showed enhancement of the thermal conductivity by about four to ten times. Wang et al. [58] showed also the improvement in thermal conductivity of paraffin wax between 35% and 40% in the addition of carbon nano tubes from 1% to 2%, respectively. Teng and Yu [59] reported enhancement of thermal conductivity by mixing paraffin wax with nanoparticles. Mills et al. [60] studied graphite matrix as a paraffin wax and results showed improvement of the thermal conductivity by order of 20–60. Zeng et al. [61] concluded that the addition of 58.9 wt.% of copper nano particles can enhance the thermal conductivity of tetra decanolasan organic PCM by an order of 9. Babapoor and Karimi [62] showed that the Al_2O_3 nanoparticles have a significant potential for enhancing the thermal conductivity of the paraffin wax.

Based on the early discussions, the practice of nanoadditives to enhance thermal conductivity of PW is rarely investigated. This outcome is in consistence with the conclusion of Lin and Al-Kayiem [63] who stated that the literature suffers a lack in the enhancement of paraffin wax by nanoadditives. The main objective of the present work is to investigate the addition of copper nanoadditive into PW and examine such storage system in solar desalinations. The study also impacted on the promotion and optimization of solar distillation process towards improving the performance of desalination and its related productivity. To fulfill this aim, experiments are conducted using three simple type solar distillers: first one is a simple type without any modifications, second one contains a PW integrated with a tube-type heat exchanger, and the third one is also equipped with heat exchanger but with Cu-PW nanocomposite (NCPW).

2. Experiments

In this section the experimental setup and measurements are described. The experimental setup contains three solar distillers of all in a simple type. All solar distillers are designed and manufactured at same dimensions and specifications. Each solar distiller is a box having a pool of water at the bottom and an inclined glass cover on the top, as shown in Fig. 1. The pool of water or the basin is made of iron material with rectangular dimension of 80 cm × 140 cm and height of 72 cm for one side, while the opposite side is at 12 cm. The inside surface of basin is coated with a black paint to increase the absorptivity of solar radiation. The outside surface of basin is insulated by a wooden plat with 1 cm thick and a gap of 2 cm between the wooden plat and the metal box. The gap is filled with a glass wall as effective insulation. A commercial glass of thickness 3 mm covers the top of the basin. The silicon is used as a thread to close any gap between the basin metal and the glass cover. Due to tendency of the glass cover, condensate water accumulates on the underside of the glass cover plate and then it is assembled with a calibrated beaker. Further specifications of distiller are presented in Table 1.

In the present work three solar distillers are used, as mentioned early, in order to examine different approaches. Fig. 2 shows a schematic diagram of the three solar stills. The first distiller is a simple type without any changes; the second one is a modified solar still by adding copper tube heat exchanger filled with PW, while the third one is like the second one but with the addition of Copper-PW nanocomposite in the tube heat exchanger instead of the PW. Each tube of the heat exchanger after filled by the PW or Copper-PW nanocomposite is closed from its both ends by

Fig. 1. Photographic view of a single type basin solar still with/without paraffin wax (PW).

Table 1
Specifications of a simple type solar still applied in this study.

Specification	Description	Dimension
Glass covers	Window glass	3 mm thickness
Frame	Wood	5 cm thickness
Basin	Iron	80 cm × 140 cm
Insulation	Glass wool	20 mm thickness
Coating	Black paint	–
PCM storage pipe	Copper	∅16 mm, L = 115 cm, thickness = 1.5 mm
PCM	Paraffin wax	2.2 kg
Nano-Cu powder	20-nm size	40 g

two copper copes. Fourteen copper tubes with the dimension of 115 cm length, 16 mm diameter and 1.5 mm material thickness, for each, are applied and placed onto the basing, as shown in Fig. 1. Fig. 3 shows a photographic view of the tube heat exchanger.

The phase change material used in this work is a paraffin wax (also called *n*-octadecaneandn–hexadecane); its characteristics and physical specifications are summarized in Table 2 [1,27,64,65]. The paraffin wax is selected because of its many advantages as its relatively high latent heat with a stable performance, nontoxicity, noncorrosivity, high density, minor change in volume during phase change, low degree of super cooling, low degradation, chemically stable, non-flammable, easily available and inexpensive. Currently, there are several types of paraffin wax available. The type chosen here is based on the characteristics and properties of the working conditions. In particular, the melting temperature of the chosen PW is about 60.5 °C, which is suitable to our environment and operating temperatures. Such paraffin wax is available in two forms: chunk or pellet. The one considered here is the pellet form with size of 5 mm diameter, as shown in Fig. 3. Such form is recommended because it is easily filled into the tube heat exchanger and simply mixed with copper nanocomposite, unlike the chunk form. The copper nanoparticles are prepared by grinding copper block and presented in a nonspherical shape, as shown in Fig. 3, with sizes from 15 nm to 25 nm. The copper was chosen as nanoadditive because of its superior thermal conductivity, which can significantly enhance the thermal conductivity of PW. The copper nanoparticles are mixed at a rate of 2% with 98% for paraffin wax; this rate was applied based on that the most recommended weight ratios of nanoadditives are in the range between 0.2% and 4% [53,66]. The properties of the paraffin wax with 2.0 wt.% nano-copper are presented in Table 2.

The calculated paraffin wax required to fill up the tube heat exchanger is about 2 kg. Such amount of paraffin wax is increased by 20 g because of its normal shrinkage by 12% of its original volume, while its phase is changed from liquid to solid [27]. Such extra PW (20 g) is needed to ensure a good surface contact between the PW/NCPW and the tube heat exchanger, i.e., good conduction/convection heat transfer process between the PW/NCPW and the saline water outside the heat exchanger. In brief, a total of 2.2 kg of paraffin wax was used as PCM to fill up the tube heat exchanger. After preparing the tube heat exchanger and filled with PW or Cu-PW nanocomposite, the tubes are closed tightly from both ends to be like encapsulation and then placed into the basin (for the second and third distillers only), as shown in Fig. 1. Such encapsulation is a practical method to prevent PW/Cu-PW to be mixed with the saline water. Then, saline water is supplied into the basin at volume of 7 L; such amount can completely cover the tube heat exchanger. Hereafter, the solar stills are positioned in a direction facing the sun radiation.

The experiments are carried out from 10:00 am until 21:00 pm. This period is applied based on the need to test the water productivity and performance of different configurations of solar stills at the attendance and absence of solar energy. During this period, different measurements are carried every half an hour, including the productivity of fresh water, solar radiation, ambient temperature, glass cover temperature, saline water temperature, PW/NCPW temperature and hot air temperature (inside the still). Such measurements are carried out using appropriate measuring instruments and devices (such as thermocouples and pyrometers), as shown in Fig. 2. Furthermore, the errors in the instruments and devices are calculated and their effects on results accuracy are considered, according to the procedure developed by Brastad and Zhen [67]. It is found that the maximum experimental error is about ±2.4%, as shown in Table 3, which is very low; furthermore, each measurement case is repeated and the average values are considered as final results. Besides, the still productivity is showed depending on some parameters like basin water depth, glass cover material, still's dimensions and its inclination [68]; hence, all these factors were maintained, while the experiments are carried out, i.e., without the back effect of other parameters.

The scenario of experiments could be summarized as follow. During daytime, the sun energy goes completely for water desalination process of regular solar still (without heat exchanger). However, in solar stills with PW/NCPW energy storage, only a portion of the solar radiation will heat the water in the basin, but the rest of

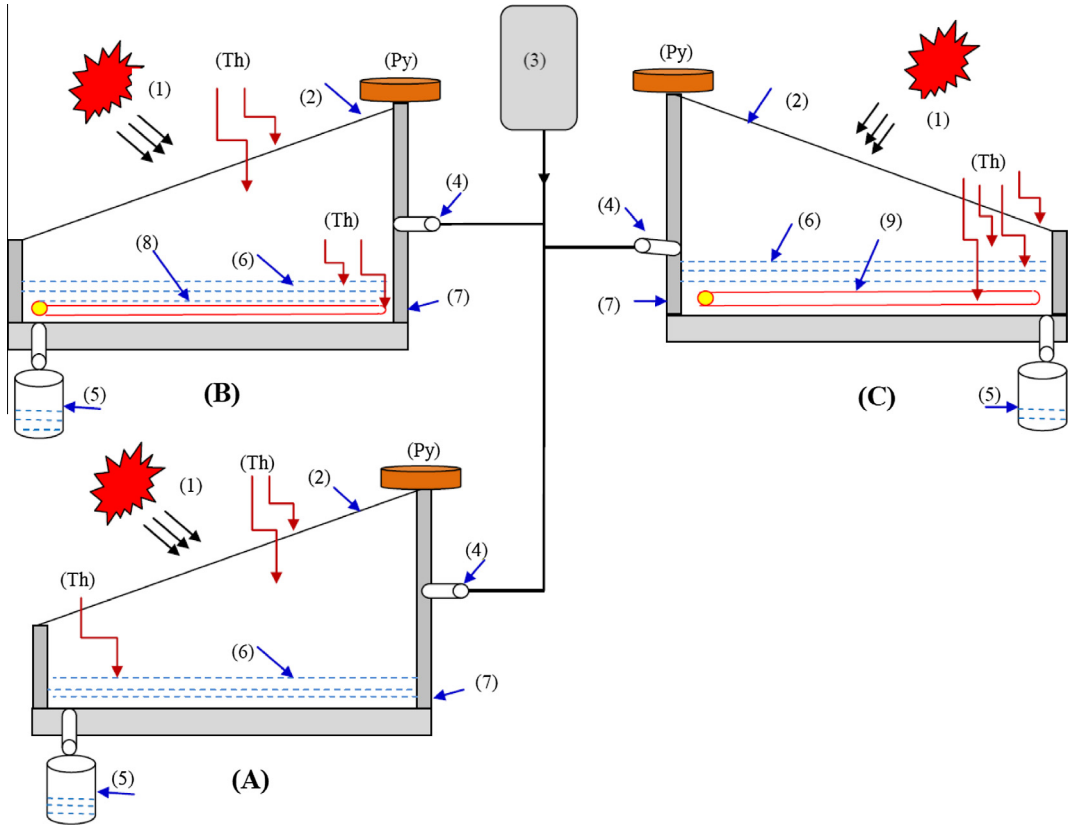

Fig. 2. A schematic diagram of a single type basin solar still in three configurations: (A) without paraffin wax (PW), (B) with PW, and (C) with Cu-PW nanocomposite (NCPW); (1) Solar radiation; (2) Glass cover; (3) Saline water tank; (4) Saline water inlet; (5) Condensed water beaker; (6) Basin; (7) Insulation; (8) Copper tube with PW; (9) Copper tube with NCPW; (Th) Thermocouples to measure temperatures of basin water, PW, hot air inside still and glass cover; (Py) Pyrometer.

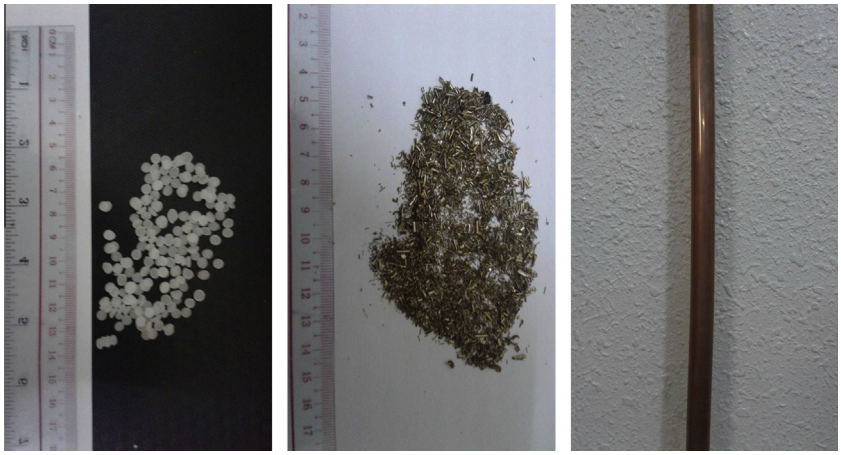

Fig. 3. Photographic views of paraffin wax at left, copper nanocomposite at middle and copper tube at right.

solar radiation will melt the PW/NCPW as a process for charging. After complete melting of the PW/NCPW, the solar energy will go completely for the water desalination process, i.e. only for heating the water. The case remains until the solar radiation near sunset. During the nighttime, solar still without heat exchanger has no source of energy; however, in the other two solar stills the PW/NCPW releases the stored thermal energy to heat up the water for continuing the desalination process, i.e., the discharging process occurs in such solar stills. For this reason, the measurements are carried out until late time of the day (21:00 pm) in order to measure the impact of PW/NCPW on water productivity and performance, compared to regular solar still without storage energy.

3. Results and discussions

The experimental results of performance and productivity of a simple type solar still at different configurations, e.g., without paraffin wax (PW), with PW and with 2.0 wt.% nano-Cu in PW (NCPW), are presented in Figs. 4–9. The results provide water productivity, intensity of solar radiation, ambient air temperature (outside distiller), glass cover temperature, hot air temperature inside distiller, basin water temperature, and phase-change material temperature at every half an hour over a day period from ten O'clock in the morning to nine O'clock in the evening. In details, Fig. 4 shows the solar radiation intensity with time. As sees, the

Table 2
Thermophysical properties of the paraffin wax (PW), Cu-PW nanocomposite (NCPW) and copper material (Cu) [1,27,64,65].

Thermophysical properties	Storage medium		
	PW	NCPW	Cu
Melting temperature (°C)	60.5	59.6	–
Solidification temperature (°C)	58.7	58.4	–
Latent heat (kJ/kg)	166.7	160.3	–
Specific heat, solid phase (kJ/kg °C)	1905	1850	381
Specific heat, liquid phase (kJ/kg °C)	2200	2100	–
Thermal conductivity (W/m °C)	0.172	0.226	387.6
Density (kg/m^3)	908.6	976.5	8978
Thermal expansion coefficient (1/K)	0.001	–	–
Dynamic Viscosity (kg/m s)	0.03499	–	–
Heat of fusion (kJ/kg)	226	–	–

solar radiation gradually increases during daytime from morning till noon, and then it gradually decreases for the rest of the day. The maximum solar radiation is about 950 W/m^2 at 13:30 pm, which has the experience of a typical moderate solar intensity in winter time.

Fig. 5 shows the variation of the following parameters through the day, the hot air temperature inside distiller, NCPW temperature, glass cover temperature, environment temperature, and basin water temperature for the distiller configuration of case 3 (with NCPW). As seen, all temperatures rise with time, starting from the early hours in the morning up to the maximum value at the time between 13:00 h and 14:00 h and then temperatures go down by the rest of the day. The s also indicated that the temperature of the basin water is higher than that of the hot air by about 10 °C, in average basis, and the temperature of the hot air is averagely higher than that of the glass cover by about 5 °C; as well, the temperature of the glass cover is averagely higher than that of the environment by about 17 °C, while the temperature of the NCPW fluctuates between higher and lower than that of the water; these differences in temperatures of dissimilar parameters are mainly due to the different heat capacities of the materials. One more note from the figure is that the peak temperature of glass cover showed some delay compared to other temperatures, i.e., glass cover, hot air, water and environment. In addition, the temperature of NCPW shows almost a flat trend for time duration between 13:30 h and 14:30 h. This is also a result of the thermal capacity differences between these materials; further discussion will be shown later. The results also indicated that the margin between temperatures of such parameters is greater during daylight hours than during night; in particular, environment, glass cover and hot air temperatures are very close at the timing of 21:00 h; also water and NCPW temperatures are close to each other. This may refer to that the heat transfer rate between the materials at this period of time tends to thermal balance condition.

Fig. 6 shows a thermal analysis of the different solar still configurations by comparison of their system temperatures, as hot air and water temperatures for case 1 (without PW), case 2 (with PW) and case 3 (with NCPW). As seen, the trends of all temperatures are in the same order with different magnitudes; the temperatures are gradually increased until they reach their maximum values in the midday and afterward they gradually decrease. Such trends are as similar as the trend of the solar radiation (Fig. 4). The maximum values of basin water and hot air temperatures, for case 3, are in the order of 58.5 °C and 52 °C, respectively, while those for the case 2 are about 60 °C and 54 °C, and those for the case 1 are about 60.5 °C and 54.5 °C, respectively. Such numbers can emphasize that the temperatures of water and hot air in case 1, for the timing before 13:30 pm, are higher than those in cases 2 and 3, while the water and hot air in case 2 are higher than those in case 3; for the time after 13:30 pm, the measurements show dissimilar trends where the water and hot air in case 3 becomes the highest, while water and hot air in the case 1 become the lowest and case 2 are in between. Motivations of such performance are as follows. Phase change materials (PW/NCPW) perform thermal energy storage process during the first half of the day; this is demonstrated by the temperature profiles of PW/NCPW, as shown in Fig. 7 and discuss later. This in turn leads to a drop in water and hot air temperatures in cases 2 and 3 than those in case 1. Furthermore, the air and water temperatures in case 3 show lower values than those in case 2 because of faster heat transfer process of NCPW due to its higher thermal conductivity. After timing of 13:30 pm, i.e., after peak condition of solar radiation, the PW/NCPW begins to discharge the storage heat into surrounding. Hence, water and air temperatures increase in cases 2 and 3; the discharge in case 3 is much faster than that in case 2 and, in turn, higher water and air temperatures of case 3 than those in case 2. One further observation on Fig. 6 is that the temperature of hot air is lower than the temperature of basin water. This is due to difference in heat capacity between water and air, as discussed early. It is also noted from the figure that the temperatures of water and hot air in case 1 reach the maximum limit faster than those in cases 2 and 3 by about 90 min; this may refer to the heat absorbed by the PW/NCPW during the first half of the day. In summary, the water and hot air temperatures of case 2 is higher than those for case 3 at the timing before 13:30 pm; this may refer to the effect of copper nanocomposite, which increases its thermal conductivity, as it will be shown later; hence, rate of heat storage/absorption in case 3 is faster than that in case 2. During the second half of the day (13:30 pm to 21:00 pm), water and air temperatures of case 3 are the highest because of greater rate of loosing the storage energy of NCPW than that in case 2; while case 1 shows the highest water and air temperatures at first half of the day and the least temperatures at the rest of the day due to its no existed energy storage material (PW/NCPW).

Fig. 7 shows the temperatures distribution of PW and NCPW as a function of time for case 2 and case 3, respectively. As seen, the temperatures of PW and NCPW behave as similar trend as solar radiation (Fig. 4) and other parameters, and that makes sense. The temperatures of both PW and NCPW increase gradually with time until their peak values and then they decrease subsequently. The temperatures of PW/NCPW show a rise until the timing of 13:30 pm (the intensity of solar radiation is peak); after that temperatures become almost horizontal for a while (plane temperatures) until timing of 14:00 pm (for PW) and 14:30 pm (for NCPW), which indicates that the melting of phase change materials (PW/NCPW) takes a place. The length of this period depends strongly on the heat capacity of the material (PW/NCPW) and solar radiation intensity. After timing of 14:00 pm (for PW) or 14:30 pm

Table 3
The accuracies, ranges, and errors of various measuring instruments used in the experiments.

No.	Instrument	Accuracy	Measuring range	Errors (%)
1	Thermocouple	±0.1 °C	0–100	0.5
2	Pyrometer	±1 W/m^2	0–2000 W/m^2	0.5
3	Measuring beaker	±1 ml	0–2000 ml	1

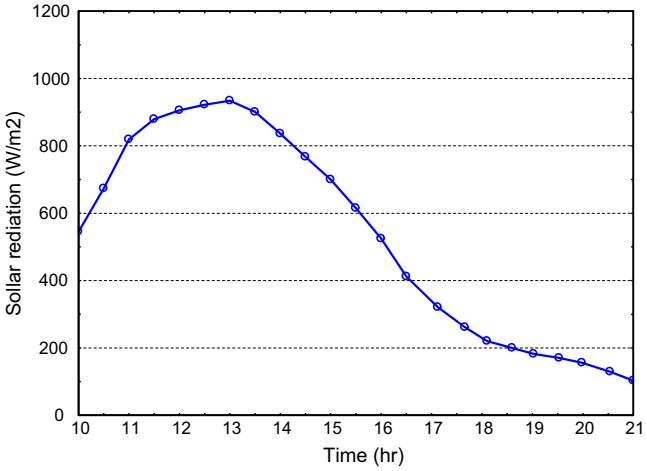

Fig. 4. Solar radiation intensity versus time.

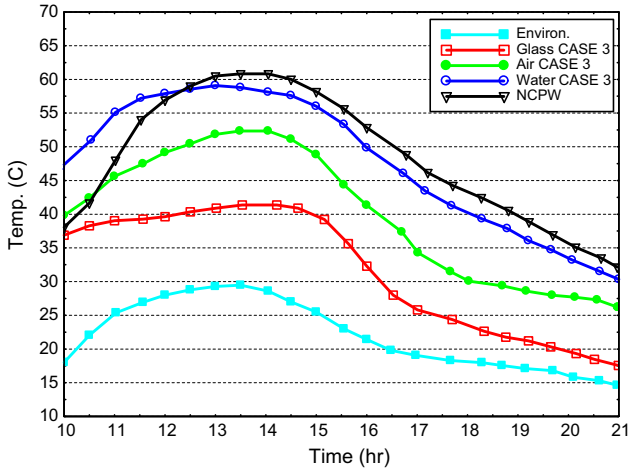

Fig. 5. Environment, air, water, glass and NCPW (Cu-PW nanocomposite) temperatures versus time for case 3.

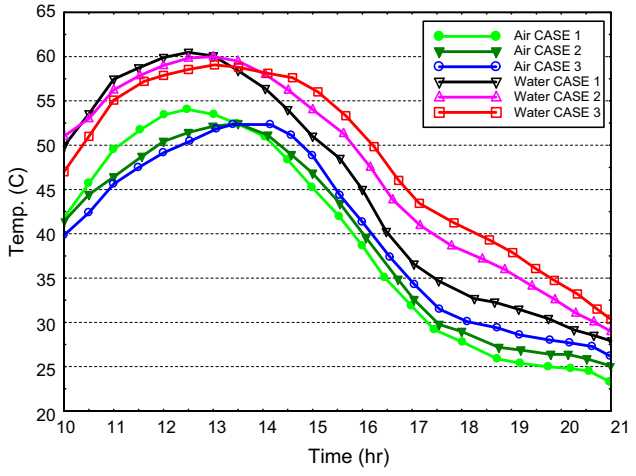

Fig. 6. Air and water temperatures versus time for case 1 without paraffin wax (PW), case 2 with PW and case 3 with Cu-PW nanocomposite (NCPW).

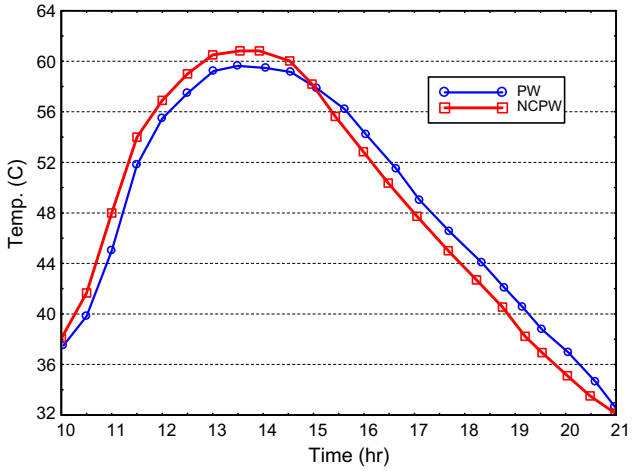

Fig. 7. Temperatures of paraffin wax (PW) and Cu-PW nanocomposite (NCPW) versus time.

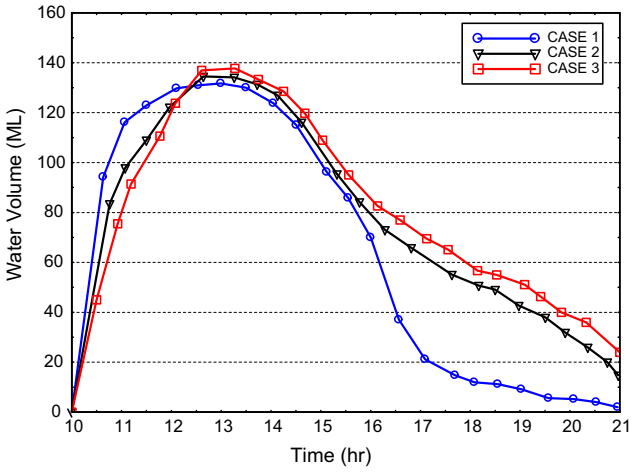

Fig. 8. Rate of water volume productivity along the day for three cases: case 1 without paraffin wax (PW), case 2 with PW, and case 3 with Cu-PW nanocomposite (NCPW).

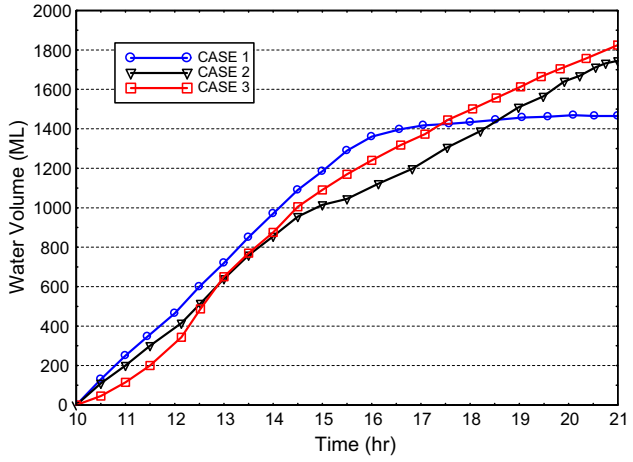

Fig. 9. Accumulated water volume productivity versus time for three cases: case 1 without paraffin wax (PW), case 2 with PW, and case 3 with Cu-PW nanocomposite (NCPW).

(for NCPW) temperatures of PW/NCPW start to decrease due to energy discharging process from the phase change materials (PW/NCPW) to water. One may also note from the figure that the temperature of NCPW is higher than that of the PW at the first half of the day but in the second half of the day the temperature of NCPW becomes lower. This is due to the impact of thermal conductivity of NCPW (0.226 W/m °C) compared to PW (0.172 W/m °C); in the first half of the day (charging period), the NCPW absorbs thermal heat faster than the PW, while in the second half (discharging process) the NCPW transfers the heat also faster to water than that of PW due to the higher thermal conductivity of NCPW. One further observation from the figure is that the peak temperature of NCPW exceeds that of PW. The reason may refer to the difference between specific heats of both PW and NCPW (1905 kJ/kg °C and 1850 kJ/kg °C for PW and NCPW in solid phase conditions, respectively, as shown in Table 2).

The temperature distribution of PW/NCPW in Fig. 7 may be divided into three zones. In the first zone, the PW/NCPW temperatures increase gradually until the melting point. In the second zone, the temperatures remain approximately constant, while the melting process of PW/NCPW takes a place, i.e. the temperatures remain constant due to latent heat. Zone three represents the release of the sensible heat stored in the liquid phase of the PW/NCPW. When we make detailed analysis on the melting process, one can emphasize that the PW/NCPW starts to melt at a layer adjacent to the contact surface of the heat exchanger. The liquid layer thickness increases as the heat transfer grows and, in turn, the temperature difference between the outer and inner layers increases. With time, the melted layer at the outer surface becomes dominant until reaching the center of the tube, i.e., completes melting. After complete melting process, the difference in temperatures between the outer and the inner layers of the PW/NCPW is diminished. At comparing the trends of PW and NCPW, we can emphasize some differences and similarities. As similarities, the method of heat transfer is a combination of natural convection and conduction in both of PW and NCPW. Besides, during the charging process, solid is melted into liquid phase and, in turn, solid–liquid interface is found in both materials. As differences, the natural convection dominates in the heat transfer process of PW at melting condition, while it is by conduction in the NCPW. In particular, heat transfer in the melting process of PW is initially performed by conduction and after partial melting, convection governs the heat transfer process; but conduction dominates in the general heat transfer process of NCPW due to existing of copper nanocomposite, which enhances the thermal conductivity by 24%, compared to the pure paraffin wax, as shown in Table 2. Increasing the thermal conductivity of the NCPW can improve heat diffusivity inside the material for better heat flow. One further difference between trends and, in turn, thermal process of PW and NCPW is that the heat transfer of thermal energy from the PW to water is not immediate but it requires some time to reach thermal balance. However, in case of NCPW, this process becomes faster, i.e., adding the copper nanocomposite enhances the heat transfer process. It was also shown that the melting process of NCPW is accelerated by 8%, compared to pure PW due to its faster heating process. Faster melting of NCPW leads to much heat absorbed and that slows down the saline water evaporation process, as discussed afterward.

A comparison between freshwater productivities for the three still's configurations is presented in Figs. 8 and 9. In particular, Fig. 8 provides the rates of water volume productivities and Fig. 9 provides the accumulated water volume productivities versus time for case 1 without PW, case 2 with PW and case 3 with NCPW. As shown in Fig. 8, the rates of freshwater productivities of the three cases increase from zero value at 10:00 am to the maximum values at timing between 13:00 pm and 14:00 pm and then they decrease till the end of the day. The accumulated freshwater productivity, as shown in Fig. 9, for case 1 is higher than those of case 2 and case 3 by about 9% and 12%, respectively, during the first half of the day, i.e., from 10:00 am to 13:30 pm. This is due to that during daytime, the sun energy goes completely for the water desalination process in case 1; however, in cases 2 and 3, only a fraction of the solar radiation heats the water and the rest is stored in the PW/NCPW as charging process. After complete melting of the PW/NCPW, the solar energy goes completely for the water desalination process, i.e. for heating the water. During the nighttime, solar still in case 1 has no productivity; however, the PW/NCPW releases the stored energy to the water in cases 2 and 3, i.e., continue the desalination process. The daily freshwater productivities, for cases 1, 2 and 3, respectively, are about 1465 ml, 1745 ml and 1824 ml. As seen, the daily water productivity for case 3 is higher than that for case 1 by about 25%; while the productivity in case 2 is higher than in case 1 by about 19%. Furthermore, the water productivity in the case 3 is higher than that in case 2 by about 6%; this refers to the higher thermal conductivity and heat capacity of NCPW. it is also shown from the figure that, at timing between 12:30 pm and 14:00 pm, there are no much differences in water productivities between cases 2 and 3 (see Fig. 8). This is due to that the melting process of PW/NCPW takes a place, i.e., solar radiation is absorbed by the PW/NCPW. After timing of 14:00 pm, one can note that the rate of water productivity in case 3 is the highest due to couple of reasons; firstly, the stored heat is discharged from NCPW into water, and, secondly, the higher heat capacity of NCPW, compared to PW, as shown in Table 1. In conclusion, the modified solar still with NCPW has the capability of higher water productivity than the still with PW. To end with, if one needs a faster rate of water productivity during the early hours in the day, solar still without PW is the best choice; however, if one needs a high water productivity at the end of the day, solar still with NCPW is the best choice; if one needs quite large water productivity at the end of the day with some quick water productivity during the early hours in the day, one should use solar still with PW.

In summary, considerable improvement in water productivity and performance is obtained if the Cu-PW nanocomposite storage system has been applied in solar still. The demonstrated enhancement includes the thermal properties in terms of faster absorption and releasing of the thermal energy and that is favorable for the solar energy storage. The dispersion of suspended Cu-nanoparticles results higher thermal diffusivity as faster heat transfer from water to NCPW. The addition of copper nanoadditive acts as nucleation agent to overcome thermal resistance during heat transfer processes. This is probably because the nano copper improves the physical bonding interaction between PW molecules to make a lower heat resistance [69]. Besides, the physical bonding of copper nanoparticles with paraffin wax does not disturb the chemical structure interaction and, in turn, the chemical stability of the material; in general, nano copper is a suitable additive to improve the thermal stability of PW. The results show that the nanocomposite increased the system efficiency by approximately 5%, compared to pure PW. The study also shows that adding nanomaterials to PW can not only increase thermal conductivity and system efficiency, but also thermal storage capacity. Furthermore, the rate of heat transfer and consequently the time for complete melting process are enhanced by adding of copper nanocomposite (the total melting time decreases by 7%). The system working time increased during night time by 5 h and 6 h when PW and NCPW are applied, respectively. The solar still heating performance and

productivity at using NCPW enhanced by about 3%, and 25%, respectively, compared to the case without PW.

4. Conclusions

This paper experimentally investigates the practice of paraffin wax (PW) as a solar energy storage material integrated with a copper nanocomposite for enhancing its thermal conductivity. Three cases were studied: case 1 without PW, case 2 with PW, and case 3 with Cu-PW nanocomposite (NCPW). Effects of nanocomposite and PW on water productivity and performance of the still's systems have been examined. Based on the findings, the following conclusions are drawn:

- The energy produced during sunshine time is stored efficiently in PW and NCPW for use later during the night; the NCPW is showed more efficient energy storage than the PW.
- The water productivity in case 3 is lower than those in cases 1 and 2, at first half of the day; however the overall daily productivity in case 3 is increased by 125% and 106%, compared to cases 1 and 2, respectively.
- The daily water productivity in case 2 is higher than that in case 1 by about 19%.
- NCPW is recommended as an effective energy storage material in simple-type solar still.
- The thermal conductivity of the NCPW was enhanced compared to the PW.
- Using nanocomposite can enhance the storage capacity of PW.
- The peak temperature of NCPW exceeds that of PW.
- The melting process of NCPW is accelerated by 7%, compared to pure PW.
- The temperature of saline water in case 1 reaches the maximum limit faster than those in cases 2 and 3 by about 1.5 h.
- Case 3 shows the least saline water temperature at first half of the day and the highest value at the rest of the day; case 1 showed the opposed result of case 3, while case 2 comes in between.
- The Cu-PW nanocomposite demonstrated enhancement in the thermal properties of PW.
- The nanocomposite increased the system efficiency by 5%, compared to pure PW.
- Adding nanomaterials to PW can not only increase thermal conductivity and system efficiency, but also thermal storage capacity.
- The system working time increased during night by 5 h and 6 h at using PW and NCPW, respectively.

References

[1] Dashtban M, Tabrizi F. Thermal analysis of a weir-type cascade solar still integrated with PCM storage. Desalination 2011;279:415–22.
[2] Kavvadias KC, Khamis I. Sensitivity analysis and probabilistic assessment of seawater desalination costs fueled by nuclear and fossil fuel. Energy Policy 2014;74:24–30.
[3] Stuber MD. Optimal design of fossil-solar hybrid thermal desalination for saline agricultural drainage water reuse. Renew Energy 2016;89:552–63.
[4] Tian L, Guo J, Tang Y, Cao L. Historical opportunity: economic competitiveness of seawater desalination project between nuclear and fossil fuel while the world oil price over $50 per barrel—Part A: MSF. Desalination 2005;183:317–25.
[5] Xiao G, Wang X, Mingjiang N, Wang F, Zhu W, Luo Z, Cen K. A review on solar stills for brine desalination. Appl Energy 2013;103:642–52.
[6] Shadi M, Abujazar S, Fatihah S, Rakmi AR, Shahrom MZ. The effects of design parameters on productivity performance of a solar still for seawater desalination: a review. Desalination 2016;385:178–93.
[7] Elfasakhany A, Mahrous AF. Performance and emissions assessment of n-butanol–methanol–gasoline blends as a fuel in spark-ignition engines. Alex Eng J 2016. http://dx.doi.org/10.1016/j.aej.2016.05.016 [in press].
[8] Elfasakhany A. Investigation on performance and emissions characteristics of an internal combustion engine fuelled with petroleum gasoline and a hybrid methanol–gasoline fuel. J Eng Technol 2013;13:24–43.
[9] Elfasakhany A. The effects of ethanol–gasoline blends on performance and exhaust emission characteristics of spark ignition engines. Int J Autom Eng 2014;4:608–20.
[10] Elfasakhany A. Investigations on the effects of ethanol–methanol–gasoline blends in a spark-ignition engine: performance and emissions analysis. Eng Sci Technol JESTECH 2015;18:713–9.
[11] Elfasakhany A. Experimental study on emissions and performance of an internal combustion engine fueled with gasoline and gasoline/n-butanol blends. Energy Convers Manage 2014;88:277–83.
[12] Elfasakhany A. Experimental investigation on SI engine using gasoline and a hybrid iso-butanol/gasoline fuel. Energy Convers Manage 2015;95:398–405.
[13] Elfasakhany A. Experimental study of dual n-butanol and iso-butanol additives on spark-ignition engine performance and emissions. Fuel 2016;163:166–74.
[14] Elfasakhany A. Performance and emissions analysis on using acetone–gasoline fuel blends in spark ignition engine. Eng Sci Technol JESTECH 2016;19:1224–32.
[15] Abdel Salam MR M.Sc. thesis. Kassel (Germany): Kassel University; 2011.
[16] Chaichan MT, Kazem HA. Water solar distiller productivity enhancement using concentrating solar water heater and phase change material (PCM). Case Stud Therm Eng 2015;5:151–9.
[17] Hermosillo J, Arancibia-Bulnes CA, Estrada CA. Water desalination by air humidification: Mathematical model and experimental study. Sol Energy 2012;86:1070–6.
[18] Farhat A, Ahmad F, Arafat H. Analytical techniques for boron quantification supporting desalination processes: a review. Desalination 2013;310:9–17.
[19] Skiborowski M, Mhamdi A, Kraemer K, Marquardt W. Model-based structural optimization of seawater desalination plants. Desalination 2012;292:30–44.
[20] Dydo P. The effect of process parameters on boric acid transport during the electrodialytic desalination of aqueous solutions containing selected salts. Desalination 2013;310:43–9.
[21] Zak GM, Mancini ND, Mitsos A. Integration of thermal desalination methods with membrane-based oxy-combustion power cycles. Desalination 2013;311:137–49.
[22] Zhang W, Mossad M, Zou L. A study of the long-term operation of capacitive deionisation in inland brackish water desalination. Desalination 2013;320:80–5.
[23] Shukla SK, Sorayan V. Thermal modeling of solar still: an experimental validation. Renew Energy 2005;30:683–99.
[24] Tripathi R, Tiwari GN. Thermal modeling of passive and active solar stills for different depths of water by using the concept of solar fraction. Sol Energy 2006;80:956–67.
[25] Velmurugan V, Kumar KJ, Haq TN, Srithar K. Performance analysis in stepped solar still for effluent desalination. Energy 2009;34:1–8.
[26] Fath HE. Technical assessment of solar thermal energy storage technologies. Renew Energy 1998;14:35–40.
[27] Al-Kayiem H, Lin SC. Performance evaluation of a solar water heater integrated with a PCM nanocomposite TES at various inclinations. Sol Energy 2014;109:82–92.
[28] Mettaweea ES, Assassa GM. Experimental study of a compact PCM solar collector. Energy 2006;31:2958–68.
[29] Summers EK, Antar MA, Lienhard JH. Design and optimization of an air heating solar collector with integrated phase change material energy storage for use in humidification–dehumidification desalination. Sol Energy 2012;86:3417–29.
[30] Ansari O, Asbik M, Bah A, Arbaoui A, Khmou A. Desalination of the brackish water using a passive solar still with a heat energy storage system. Desalination 2013;324:10–20.
[31] Abdallah S, Abu-Khader M, Badran O. Effect of various absorbing materials on the thermal performance of solar stills. Desalination 2009;242:128–37.
[32] Radhwan AM. Transient performance of a stepped solar still with built-in latent heat thermal energy storage. Desalination 2004;171:61–76.
[33] El-Sebaii A, Al-Ghamdi A, Al-Hazmi FS, Faidah AS. Thermal performance of a single basin solar still with PCM as a storage medium. Appl Energy 2009;86:1187–95.
[34] Kurklu A, zmerzi AO, Bilgin S. Thermal performance of a water-phase change material solar collector. Renew Energy 2002;26:391–9.
[35] Khalifa AJ, Suffer KH, Mahmoud MS. A storage domestic solar hot water system with a back layer of phase change material. Exp Therm Fluid Sci 2013;44:174–81.
[36] Al-Hinti I, Al-Ghandoor A, Maaly A, Abu-Naqeera I, Al-Khateeb Z, Al-Sheikh O. Experimental investigation on the use of water-phase change material storage in conventional solar water heating systems. Energy Convers Manage 2010;51:1735–40.
[37] Bouadila S, Fteiti M, Ouslati M, Guizani A, Farhat A. Enhancement of latent heat storage in a rectangular cavity: solar water heater case study. Energy Convers Manage 2014;78:904–12.
[38] Wei J, Kawaguchi Y, Hirano S, Takeuchi H. Study on a PCM heat storage system for rapid heat supply. Appl Therm Energy 2005;25:2900–20.
[39] Shukla A, Buddhi D, Sawhney RL. Thermal cycling of few selected inorganic & organic phase change materials. Renew Energy 2008;33:2606–14.
[40] Elfasakhany A, Kassem TK, Mahrous A-F, Matrawy KK. Study of heat storage using of PCM in solar distiller. WULFENIA 2016;23:19–31.
[41] van Miltenburg JC, Onk HA, Metivaud V. Heat capacities and derived thermodynamic functions of n-nonadecane and n-eicosane between 10 K and 390 K. J Chem Eng Data 1999;44:715–20.

[42] Hawlader MN, Uddin MS, Zhu HJ. Encapsulated phase change materials for thermal energy storage: experiments and simulation. Energy Res 2002;26:159–71.
[43] He B, Setterwall F. Technical grade paraffin waxes as phase change materials for cool thermal storage and cool storage systems capital cost estimation. Energy Convers Manage 2002;43:1709–23.
[44] Rao Z, Wang S, Wu M, Zhang Y, Li F. Molecular dynamics simulations of melting behavior of alkane as phase change materials slurry. Energy Convers Manage 2012;64:152–6.
[45] Sigel R. Solidification of low conductivity material containing dispersed high conductivity particles. J Heat Mass Transfer 1977;20:1087–9.
[46] Khodadadi JM, Hosseinizadeh SF. Nanoparticle-enhanced phase change materials (NEPCM) with great potential for improved thermal energy storage. Int Commun Heat Mass Transfer 2007;34:534–43.
[47] Hawlader MNA, Uddin MS, Khin MM. Microencapsulated PCM thermalenergy storage system. Appl Energy 2003;74:195–202.
[48] Tyagi VV, Kaushik SC, Tyagi SK, Akiyama T. Development of phase change materials based microencapsulated technology for buildings: a review. Renew Sustain Energy Rev 2011;15:373–1391.
[49] Tong X, Khan JA, Amin MR. Enhancement of heat transfer by inserting a metal matrix into a phase change material. Num Heat Transfer – Part A 1996;30:125–41.
[50] Zhao CY, Lu W, Tian Y. Heat transfer enhancement for thermal energy storage using metal foams embedded within phase change materials (PCMs). Sol Energy 2010;84:1402–12.
[51] Mehling H. Latent heat storage with a PCM–graphite composite material: experimental results from the first test store. In: Proceedings of the 6th workshop of IEA, Stockholm, Sweden.
[52] Zhang ZG, Zhang N, Peng J, Fang XM, Gao XN, Fang YT. Preparation and thermal energy storage properties of paraffin/expanded graphite composite phase change material. Appl Energy 2012;91:426–31.
[53] Wang JF, Xie HQ, Xin Z. Thermal properties of paraffin based composites containing multi-walled carbon nanotubes. Thermochem Acta 2009;488:39–42.
[54] Mei D, Zhang B, Liu RC, Zhang YT, Liu JD. Preparation of capric acid/halloysite nanotubes composite as form-stable phase change material for thermal energy storage. Sol Energy Mater Sol Cells 2011;95:2772–7.
[55] Fukai J, Hamada Y, Morozumi Y, Miyatake O. Improvement of thermal characteristics of latent heat thermal energy storage units using carbon-fiber brushes: experiments and modeling. Heat Mass Transfer 2003;46:4513–25.
[56] Frusteri F, Leonardi V, Vasta S, Restuccia G. Thermal conductivity measurement of a PCM based storage system containing carbon fibers. Appl Therm Eng 2005;25:1623–33.
[57] Ho CJ, Gao TY. Preparation and thermophysical properties of nanoparticle in paraffin emulsion as phase change material. Int Commun Heat Mass Transfer 2009;36:467–70.
[58] Wang J, Xie H, Guo Z, Li Y. Improved thermal properties of paraffin wax by the addition of TiO_2 nanoparticles. Appl Therm Eng 2014;73:1541–7.
[59] Teng TP, Yu CC. Characteristics of phase-change materials containing oxide nano-additives for thermal storage. Nanoscale Res Lett 2012;7:611–21.
[60] Mills A, Farid M, Selman JR, Al-Hallaj S. Thermal conductivity enhancement of phase change materials using a graphite matrix. Appl Therm Eng 2006;26:1652–61.
[61] Zeng LJ, Zhua FR, Yub SB, Zhua L, Caoa Z, Suna LX, Denga GR. Effects of copper nano wires on the properties of an organic phase change material. Sol Energy Mater Sol Cells 2012;105:174–8.
[62] Babapoor A, Karimi G. Thermal properties measurement and heat storage analysis of paraffin nanoparticles composites phase change material: comparison and optimization. Appl Therm Eng 2015;90:945–51.
[63] Lin SC, Al-Kayiem H. Evaluation of copper nanoparticles – paraffin wax compositions for solar thermal energy storage. Sol Energy 2016;132:267–78.
[64] Haji-Sheikh A, Eftekhar J, Lou DY. Some thermophysical properties of paraffin wax as a thermal storage medium. American Institute of Aeronautics and Astronautics; 1982.
[65] Al-Abidi A, Mat S, Sopian K, Sulaiman MY, Mohammad A. Numerical study of PCM solidification in a triplex tube heat exchanger with internal and external fins. Heat Mass Transfer 2013;61:684–95.
[66] Cai Y, Ke H, Dong J, Wei Q, Lin J, Zhao Y, Song L, Hu Y, Huang F, Gao W, Fong H. Effect of nano-SiO_2 on morphology, thermal energy storage, thermal stability and combustion properties of electrospunlauric acid/PET ultrafine composite fibres as form-stable phase change materials. Appl Energy 2011;88:2106–12.
[67] Brastad KS, Zhen H. Water softening using microbial desalination cell technology. Desalination 2013;309:32–7.
[68] El-Bialy E. Performance analysis for passive single slope single basin solar distiller with a floating absorber: an experimental study. Energy 2014;68:117–24.
[69] Xiang J, Drzal LT. Investigation of exfoliated graphite nano platelets (xGnP) in improving thermal conductivity of paraffin-based phase change material. Sol Energy Mater Sol Cells 2011;95:1811–8.